

# Transceiver Impairments Compensation via Deep Learning for High Baud-Rate Coherent Systems

José Hélio da Cruz Júnior, Joaquim Ferreira Martins Filho, Raul Camelo de Andrade Almeida Júnior, Rafael Carvalho Figueiredo and Leonardo Didier Coelho

**Abstract**—In this paper, we propose a transceiver impairments compensation method employing deep learning equalization for high baud-rate coherent optical systems. The method is based on a deep cascade-forward neural network. The performance evaluation of the nonlinear equalizer was carried out through numerical simulations based on back-to-back optical transmission considering a 1.2 Tb/s line rate single wavelength (DP-16QAM at 150 Gb/s). The results indicate that the proposed equalization achieves optical signal-to-noise ratio (OSNR) gains equal to 0.5 and 2 dB compared with the conventional deep feed-forward neural network and linear cases, respectively. The proposed equalizer also presents data rate gains, compared with the conventional deep neural network and linear, respectively, equal to 50 and 150 Gb/s, in the low OSNR regime, and 10 and 70 Gb/s, for the high OSNR regime. Moreover, the impact of equalizer architecture aspects is analyzed. The simulation results confirm that the proposed equalization technique is a good solution to mitigate linear and nonlinear transceiver distortions enabling the next generation of 1 Tb/s coherent modules.

**Keywords**—Transceiver impairments compensation, deep learning, deep cascade-forward neural network, high baud-rate coherent systems.

## I. INTRODUCTION

In order to satisfy the demand of Internet connectivity, the optical communications systems industry urge for high-capacity and cost-effective solutions over a wide range of applications such as submarine, terrestrial long-haul, metro and access networks, for traditional telecom services providers (TSP), and data center interconnect (DCI), for cloud services providers (CSP). In this way, the coherent line interfaces continue to evolve the transmission rate per wavelength from 100 Gb/s to 800 Gb/s in commercial systems [1]. As 100/200 Gb/s optical systems are well commercially established [2], the 400/600 Gb/s systems are presenting an impressive growth in deployments [3], boosted mainly by standards and multi-source agreement (MSA) such as 400ZR, Open ROADM and OpenZR+ [4]. Regarding the 800 Gb/s coherent transceivers, it is expected a massive adoption in the next years, also accelerated by future standards such as 800ZR [1]. To support the growing traffic demands, the next frontier in coherent technology pushes the single wavelength capacity towards 1 Tb/s [5], [6].

J. H. Cruz Júnior, J. F. Martins Filho, R. C. A. Almeida Júnior and L. Didier Coelho are with the Department of Electronics and Systems (DES), Federal University of Pernambuco (UFPE), Recife-PE, e-mail: joseheliiodacruzjunior@gmail.com; joaquim.martins@ufpe.br; raul.almeidajunior@ufpe.br; leonardo.coelho@ufpe.br; R. C. Figueiredo is with the Optical Communication Solutions, CPQD, Campinas-SP, e-mail: rafaelcf@cpqd.com.br.

This work was supported by FACEPE.

To achieve a high transmission rate per wavelength as 1 Tb/s, the main physical degrees of freedom to explore in a coherent optical transceiver are the number of optical subcarriers, modulation format, and symbol rate. Regarding the first, single-carrier approaches come up as an attractive solution compared with multi-carrier implementations due to the reduced transceiver complexity and cost [7]. Specifically for a single-carrier solution, the combination of high-order quadrature amplitude modulation (QAM) format, as the dual-polarization (DP) 16QAM in contrast with DP-64QAM, and high baud rate, currently, is the best option to scale the bit rate of a coherent line interface, yielding to a reasonable trade-off between implementation cost and system performance [8]. Nevertheless, optical systems based on high-order QAM modulation and high symbol rate are highly impacted by optical fiber nonlinear distortions, noise sources and transceiver impairments such as linear and nonlinear distortions of electrical components, including digital-to-analog and analog-to-digital converters (DAC and ADC), driver, and transimpedance amplifiers (DA and TIA), and optical components, such as modulators and photodetectors [9].

Recent advances in digital electronics enabled the development of application specific integrated circuits (ASICs) for coherent optical transceivers. The main digital signal processing (DSP) blocks implemented in the coherent ASICs are the linear equalizers to compensate linear impairments such as chromatic dispersion (CD) and polarization mode dispersion (PMD). Now, efforts are made to mitigate nonlinear effects imposed by the optical fiber such as self-phase modulation (SPM), cross-phase modulation (XPM) and four-wave mixing (FWM) [10] and also distortions imposed by the transmitter and receiver and, among them, the deep learning equalization has been a promising solution [11].

Several works exploring deep learning methods, precisely deep neural networks (DNN), have been reported. In [12], a nonlinear equalizer based on a complex-valued DNN to mitigate the nonlinear impairments caused by optical fiber propagation but also imperfections resulting from using low-cost electrical and optical front-end components is proposed. In [5], a DNN is trained to mitigate the transceiver response of a 128 GBd coherent optical system based on a training process using either a direct learning architecture (DLA) or an indirect learning architecture (ILA). In [13], a DLA-based DNN using a curriculum learning approach for transceiver impairments compensation is demonstrated. However, all the above mentioned techniques consider

complex DNN architectures, increasing the DSP complexity. Moreover, the transmitter (TX)-based digital pre-distortion (DPD) requires an iterative feedback loop for training, which affects the peak-to-average power ratio (PAPR) of the transmitted signal [14].

In this paper, we propose an alternative receiver (Rx)-based deep cascade-forward neural network (CDNN) for transceiver impairments compensation applied to high baud-rate coherent optical systems. The CDNN presents an operating principle similar to the conventional DNN, but including connections between the input/output of each layer and each subsequent layer, allowing it to improve the mapping between the input and the desired output. The proposed deep learning equalization is used in the Rx DSP and presents a simple architecture, decreasing the digital receiver complexity and eliminating any iterative feedback loop for training. The performance evaluation of the nonlinear equalizer is carried out through numerical simulations based on a back-to-back optical transmission system considering single-carrier 1.2 Tb/s (DP-16QAM at 150 GBd).

## II. DEEP LEARNING EQUALIZATION

The Fig. 1(a) shows the structure of a conventional DNN used for transceiver impairments mitigation. The DNN tries to find a function that maps the input to the desired target by considering intermediate steps based on the neurons of the network. The implemented DNN comprise  $4(m + 1)$  real-valued inputs, where 4 represents the real and complex components of a dual-polarization signals and  $m$  is memory depth, and 4 real-valued outputs with  $l$  hidden-layers of  $h_l$  neurons each [9]. For each neuron, three steps are carried out: (1) weight multiplication of inputs, (2) summing the weighted inputs and a bias, and (3) passing the results of (2) through an activation function. For the proposed nonlinear equalizer, we use a network with  $m = 5$ , up to two hidden layers ( $l = 2$ ) and 15 neurons per layer ( $h_l = 15$  for all  $l$ ). The impact of different numbers of hidden layer and neurons per layer is also investigated. The activation function considered in each hidden layer is a nonlinear hyperbolic tangent sigmoid transfer function, meanwhile the output layer uses a linear transfer function.

The transceiver impairments compensation employing the DNN is based on two phases: training and evaluation. In the training step the estimation of the model parameters is performed, where initial weights and biases are applied to the training data, resulting in a certain output of the neural network, characterizing the forward propagation. The difference between the actual output and desired targets of the DNN is used to calculate a loss function. Afterwards, the gradients of the loss function are calculated considering a backward propagation. Finally, the parameters of the DNN (weights and biases) are updated based on the Levenberg-Marquardt backpropagation algorithm [15].

The training phase is performed in a specific optical signal-to-noise ratio (OSNR) equal to 27 dB (defined as calibration point). At the calibration point, one data frame is captured and used for the training process. For each OSNR

value, the evaluation phase is carried out over five data frames. This approach ensures a separation of training and evaluation data, respectively training and testing data [16]. In both phases we used data frames with  $\approx 250000$  symbols. Specifically in the training phase, the data frame was divided in two sets: 70% for the training set, which is used for computing the gradient and updating the weights and biases, and 30% for the validation set, which is used as a pre-test to avoid overfitting and underfitting. The training phase is carried out until validation error increases compared to the training error for a specified number of iterations (in order to prevent overfitting) or the maximum number of epochs (500) is reached.

In the evaluation phase, the received signals pass through the trained DNN for performance measurement considering the mean over the five data frames. An alternative to the conventional DNN is the CDNN [17]. The Fig. 1(b) shows the block diagram of a DNN with cascaded structure. The CDNN allows to improve the mapping between the input and the desired output. The neural network with a cascaded configuration presents a principle similar compared with the DNN, but includes connections between the input/output of each layer and each subsequent layer.

## III. SIMULATION MODEL

The simulation setup is presented in Fig. 2. At the Tx side, a DSP stack is employed. First, a pseudorandom binary sequence (PRBS) is generated and mapped into constellation symbols (16QAM), which are upsampled and filtered by a root-raised-cosine filter (roll-off=0.1). Following, the DAC converts the signal to the analog domain with a symbol rate equal to 150 GBd, which is sufficient to include 20%-overhead (OH) for soft-decision (SD) forward error correction (FEC), achieving a net bit rate of 1 Tb/s. Finally, the electrical signals are applied into a LiNbO<sub>3</sub> dual-polarization in-phase and quadrature modulator (DP-IQM), modulating the optical carrier. The desired OSNR at the Rx side is obtained through amplified spontaneous emission (ASE) noise insertion, allowing one to sweep the received OSNR.

At the Rx side, the received signal is detected using a polarization-diversity coherent optical receiver. The receiver comprises a 90° optical hybrid connected to a local oscillator. The four optical outputs are converted to the electrical domain using balanced photodetectors (PD). The four electrical signals are sampled by an ADC for offline processing. The DSP subsystem considering the deep learning equalization is described as follows. First, the received electrical signals are resampled to 2 samples per symbol in the pre-processing stage. Next, they are orthonormalized to compensate the optical front-end distortions and inphase and quadrature imbalances using Gram-Schmidt orthogonalization procedure (GSOP). Polarization demultiplexing is performed by radius directed equalization (RDE) (with 20 taps), where the constant modulus algorithm (CMA) is used for pre-convergence. After this, carrier recovery (CR) is employed to compensate frequency offset and phase noise using  $M^{th}$  power frequency algorithm and two-stage blind phase search (BPS) algorithm (with 30

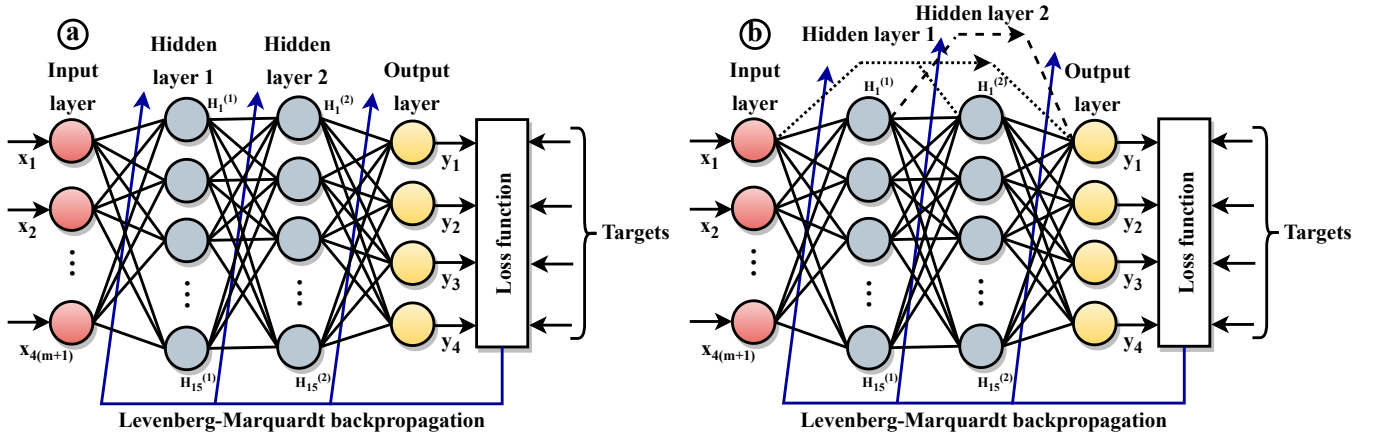


Fig. 1. Block diagrams of different nonlinear equalizers: (a) conventional deep feed-forward neural network and (b) proposed deep cascade-forward neural network.

phases per stage, window size of 100, and step size of 50). After the CR, the DNN or CDNN is applied. Finally, the error vector magnitude (EVM) is calculated, which is given by [18]:

$$\text{EVM}_{\text{rms}} = \sqrt{\frac{\sum_{n=1}^N |y_n - x_n|^2}{\sum_{n=1}^N |x_n|^2}}, \quad (1)$$

where  $y_n$  is the  $n$ -th received symbol and  $x_n$  is the  $n$ -th ideal constellation symbol. Based on the EVM, the electrical signal-to-noise ratio (SNR) is estimated by [19]:

$$\text{SNR} \approx \left[ \frac{1}{\text{EVM}_{\text{rms}}} \right]^2. \quad (2)$$

In the Shannon theory, the constrained capacity (or maximum mutual information (MI) achieved by a specific modulation format) for a discrete memoryless channel, in bit/symbol, is given by [20]:

$$C = \sum_{k=0}^{M-1} \Pr(A_k) \int_{-\infty}^{\infty} \rho_{Y|A_k}(y|A_k) \cdot \log_2 \left[ \frac{\rho_{Y|A_k}(y|A_k)}{\sum_{l=0}^{M-1} \Pr(A_l) \rho_{Y|A_l}(y|A_l)} \right] dy, \quad (3)$$

where  $\Pr(A_k)$  is the probability associated with the generation of symbol  $A_k$ , and  $\rho_{Y|A_k}(y|A_k)$  is the probability density function of the channel output given that symbol  $A_k$  was

transmitted. For a complex additive white Gaussian noise (AWGN) channel with variance  $\sigma^2$  at each dimension, the probability density function is given by:

$$\rho_{Y|A_k}(y|A_k) = \frac{1}{2\pi\sigma^2} e^{-\frac{|y-A_k|^2}{2\sigma^2}}. \quad (4)$$

Therefore, the capacity  $C$  can be related with the SNR =  $E[|A_k|^2]/(2\sigma^2)$ . The association between the electrical and optical domains is done by relating SNR and OSNR using [21]:

$$\text{SNR} = \frac{2}{p} \frac{B_n}{R_s} \text{OSNR}, \quad (5)$$

where  $p$  is the number of polarization modes,  $R_s$  is the symbol rate, and  $B_n$  the reference bandwidth (typically 0.1 nm or 12.5 GHz). Although, to include practical optical system aspects such as transceiver impairments and DSP algorithms limitations, the performance analysis is carried out replacing the theoretical curves (given by Eqs. (3) and (5)) by simulation curves generated by offline data post-processing. In this case, the OSNR was varied considering a specific range, and the electrical SNR (Eq. (2)) was estimated from the EVM (Eq. (1)) and the Gaussian assumption for the noise. After this, using the estimated electrical SNR, the MI and, consequently, the data rate (as a result of multiplying the MI by the symbol rate), assuming a capacity-achieving FEC scheme, are obtained interpolating the theoretical curve [22].

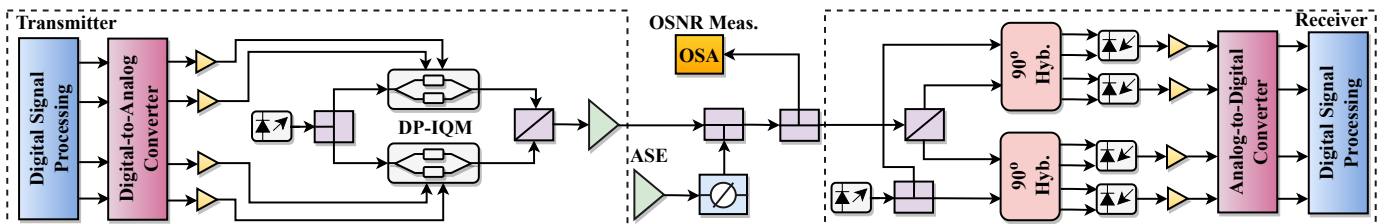


Fig. 2. Simulation setup employing an amplified spontaneous emission (ASE) noise loading method to range the received OSNR.

#### IV. SIMULATION RESULTS

The performance evaluation of the proposed nonlinear equalizer based on CDNN for transceiver impairments mitigation is carried out using the simulation setup presented in Fig. 2. The simulation parameters are listed in Table I. The electrical and optical front-end specifications considered are typically used in 800 Gb/s coherent optical transceivers, which are based on the best commercially available components [23].

TABLE I  
SIMULATION PARAMETERS.

Component	Parameter	Value
Signals	Symbol Rate	150 GBd
	Filter Roll-off	0.1
	Quantization	8 bits
DAC and ADC	Bandwidth	70 GHz
	Sample Rate	300 GSa/s
	Deterministic Jitter	1 ps
	Random Jitter	0.25 ps
	Laser Wavelength	1550 nm
Transmitter	Laser Linewidth	100 kHz
	Modulator Bandwidth	70 GHz
Receiver	Laser Linewidth	100 kHz
	PD Bandwidth	70 GHz

Figure 3 presents the data rate, obtained by the multiplication of MI and symbol rate, versus the OSNR for the proposed CDNN, conventional DNN and standard DSP without nonlinear equalization, defined here as linear DSP. As expected, in lower OSNRs, the data rate decrease as a consequence of the high ASE level. In addition, the convergence and performance of the DSP algorithms become critical, and the electrical SNR falls rapidly when the algorithms are unable to converge properly [24]. On the other side, in higher OSNRs, the data rate increases as a result of low ASE level. Curiously, the data rate is always below the maximum data rate mostly because of DAC and ADC limitations [24].

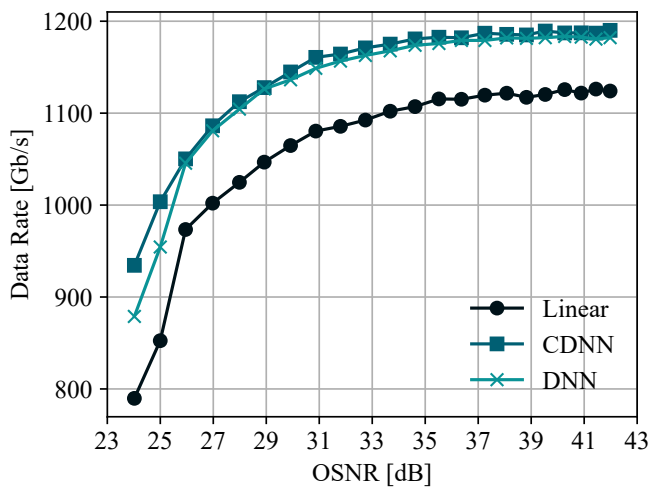


Fig. 3. Data rate versus OSNR for the CDNN, DNN and linear cases.

Considering a target data rate equal to 1 Tb/s, the CDNN presents OSNR gains equal to 0.5 and 2 dB compared with the DNN and linear cases, respectively. Also, the CDNN shows

data rate gains equal to 50 and 150 Gb/s compared with DNN and linear DSP, respectively, in the low OSNR regime (25 dB). Meanwhile, for the high OSNR regime (37 dB), the proposed nonlinear equalizer achieve data rate gains equal to 10 and 70 Gb/s in contrast to the DNN and linear, respectively. The previous results confirm that the deep learning equalizer is able to compensate the linear and nonlinear transceiver impairments improving the performance in all system operation regimes.

Figure 4 presents the data rate as a function of the OSNR for the CDNN equalizer considering two hidden layers and different numbers of neurons per layer. The equalizer architecture notation e.g., 10|10 stands two hidden layers with 10 neurons each one. The 15|15 model is used here as a benchmark. The 10|10 and 5|5 architectures shows data rate reductions, respectively, equal to 5 and 30 Gb/s, for the low OSNR regime (29 dB), and 10 e 30 Gb/s, in the high OSNR regime (37 dB).

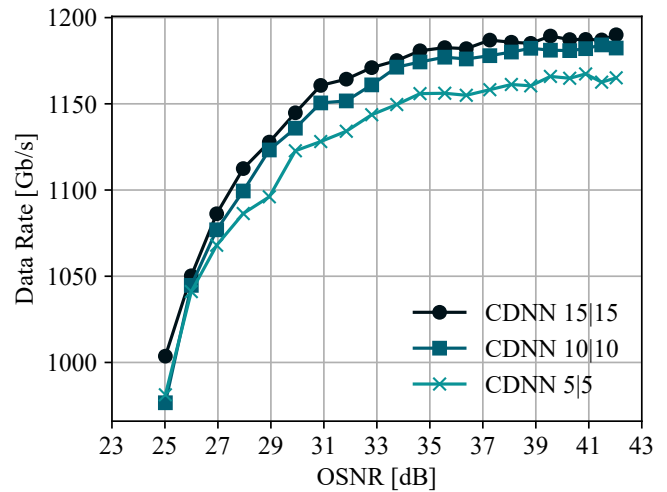


Fig. 4. Data rate versus OSNR for the proposed CDNN considering two hidden layers and different number of neurons per layer.

Figure 5 presents the data rate versus the OSNR for the CDNN equalization using one or two hidden layers and 15 neurons per layer. We use the same equalizer architecture notation depicted in Fig. 4. Again, the 15|15 model is used as benchmark. The equalizer architecture based on a single hidden layer with 15 neurons shows a data rate reduction equal to 20 Gb/s, in the low OSNR regime (29 dB), and 30 Gb/s, for the high OSNR regime (37 dB). The preceding results elucidate the impact of equalizer architecture aspects, showing the importance of a proper model design by the DSP engineer to achieve a trade-off of complexity/power consumption and performance towards an ASIC implementation.

#### V. CONCLUSIONS

We proposed a transceiver impairments compensation method employing a deep cascade-forward neural network for high baud-rate coherent optical transmission systems. The performance of the deep learning equalization was analyzed based on 1.2 Tb/s (DP-16QAM at 150 GBd) back-to-back optical transmission simulations. The simulation results

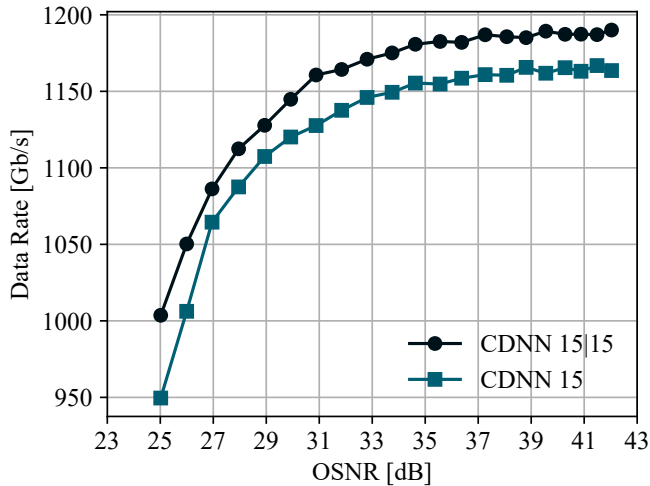


Fig. 5. Data rate versus OSNR for the proposed CDNN considering one or two hidden layers and 15 neurons per layer.

indicated that the proposed nonlinear equalizer achieved OSNR gains equal to 0.5 and 2 dB compared with the conventional DNN and linear DSP, respectively. Furthermore, the proposed method presented data rate gains, compared with the DNN and linear, respectively, equal to 50 and 150 Gb/s, in the low OSNR regime, and 10 and 70 Gb/s, for the high OSNR regime. Additionally, we investigated the influence of equalizer architecture on the performance, confirming the necessity of an appropriate equalizer design towards a practical implementation.

## REFERENCES

- [1] D. Tauber, B. Smith, D. Lewis, E. Muhigana, M. Nissov, D. Govan, J. Hu, Y. Zhou, J. Wang, W.-J. Jiang, R. Galeotti, F. Dell'Orto, and R. Siano, "Role of Coherent Systems in the Next DCI Generation," *Journal of Lightwave Technology*, vol. 41, no. 4, pp. 1139–1151, 2023.
- [2] J. Li, A. Zhang, C. Zhang, X. Huo, Q. Yang, J. Wang, J. Wang, W. Qu, Y. Wang, J. Zhang, M. Si, Z. Zhang, and X. Liu, "Field Trial of Probabilistic-Shaping-Programmable Real-Time 200-Gb/s Coherent Transceivers in an Intelligent Core Optical Network," in *Asia Communications and Photonics Conference (ACP)*, 2018.
- [3] H. Zhang, B. Zhu, T. Pfau, M. Aydinlik, N. Nadarajah, S. Park, J. C. Geyer, L. Chen, R. Aroca, C. Doerr, and C. Rasmussen, "Real-time transmission of single-carrier 400 Gb/s and 600 Gb/s 64QAM over 200km-span link," in *European Conference on Optical Communication (ECOC)*, 2019.
- [4] E. Pincemin, Y. Loussouarn, A. Sotomayor, G. Losio, M. McCarthy, L. Nelson, A. Malik, I. Riggs, T. Nielsen, T. Williams, A. Gaibazzi, L. Zhang, W. Way, F. Courchesne, and M. Vasconcellos, "End-to-End Interoperable 400-GbE Optical Communications Through 2-km 400GBASE-FR4, 8 × 100-km 400G-OpenROADM and 125-km 400-ZR Fiber Lines," *Journal of Lightwave Technology*, vol. 41, no. 4, pp. 1250–1257, 2023.
- [5] V. Bajaj, F. Buchali, M. Chagnon, S. Wahls, and V. Aref, "Deep Neural Network-Based Digital Pre-Distortion for High Baudrate Optical Coherent Transmission," *Journal of Lightwave Technology*, vol. 40, no. 3, pp. 597–606, 2022.
- [6] R. C. Figueiredo, A. Felipe, A. L. N. Souza, E. S. Rosa, F. D. Simões, F. L. Della Lucia, G. C. C. P. Simões, G. B. Farias, H. A. de Andrade, J. Hélio da Cruz, T. Sutili, Y. R. R. Bustamante, and S. M. Rossi, "Advances and Perspectives Towards Tb/s Optical Transmission (Invited Paper)," in *SBFoton International Optics and Photonics Conference (SBFoton IOPC)*, 2019.
- [7] R. Rios-Muller, J. Renaudier, L. Schmalen, and G. Charlet, "Practical approaches to 400G single-carrier submarine transmission," in *Optical Fiber Communications Conference (OFC)*, 2016.
- [8] M. Nakamura, T. Sasai, K. Saito, F. Hamaoka, T. Kobayashi, H. Yamazaki, M. Nagatani, Y. Ogiso, H. Wakita, Y. Kisaka, and Y. Miyamoto, "1.0-Tb/s/λ 3840-km and 1.2-Tb/s/λ 1280-km Transmissions with 168-GBaud PCS-QAM Signals Based on AMUX Integrated Frontend Module," in *Optical Fiber Communications Conference (OFC)*, 2022.
- [9] T. T. Nguyen, T. Zhang, E. Giacomidis, A. A. Ali, M. Tan, P. Harper, L. P. Barry, and A. D. Ellis, "Coupled Transceiver-Fiber Nonlinearity Compensation Based on Machine Learning for Probabilistic Shaping System," *Journal of Lightwave Technology*, vol. 39, no. 2, pp. 388–399, 2021.
- [10] C. Li, F. Zhang, Y. Zhu, M. Jiang, Z. Chen, and C. Yang, "Fiber Nonlinearity Mitigation in Single Carrier 400 G and 800 G Nyquist-WDM Systems," *Journal of Lightwave Technology*, vol. 36, no. 17, pp. 3707–3715, 2018.
- [11] P. J. Freire, A. Napoli, B. Spinnler, N. Costa, S. K. Turitsyn, and J. E. Prilepsy, "Neural Networks-Based Equalizers for Coherent Optical Transmission: Caveats and Pitfalls," *Journal of Selected Topics in Quantum Electronics*, vol. 28, no. 4, pp. 1–23, 2022.
- [12] P. J. Freire, V. Neskornuiuk, A. Napoli, B. Spinnler, N. Costa, G. Khanna, E. Riccardi, J. E. Prilepsy, and S. K. Turitsyn, "Complex-Valued Neural Network Design for Mitigation of Signal Distortions in Optical Links," *Journal of Lightwave Technology*, vol. 39, no. 6, pp. 1696–1705, 2021.
- [13] M. Tzur, G. Paryanti, and D. Sadot, "Statistical Wide-Sense Curriculum Learning for Neural Network-Based Pre-Distorter in Coherent Optical Transmitters," *IEEE Transactions on Communications*, vol. 70, no. 7, pp. 4513–4526, 2022.
- [14] V. Neskornuiuk, F. Buchali, V. Bajaj, S. K. Turitsyn, J. E. Prilepsy, and V. Aref, "Neural-Network-Based Nonlinearity Equalizer for 128 GBaud Coherent Transceivers," in *Optical Fiber Communications Conference (OFC)*, 2021.
- [15] M. Hagan and M. Menhaj, "Training feedforward networks with the Marquardt algorithm," *IEEE Transactions on Neural Networks*, vol. 5, no. 6, pp. 989–993, 1994.
- [16] M. Schaedler, C. Bluemm, M. Kuschnerov, F. Pittalà, S. Calabrò, and S. Pachnicke, "Deep Neural Network Equalization for Optical Short Reach Communication," *Applied Sciences*, vol. 9, pp. 33–46, 2019.
- [17] M. V. Selvi and S. Mishra, "Investigation of Weather Impact on Electric Load Power Forecasting based on Cascade Forward Neural Network Technique," in *International Conference on Computing Communication and Automation (ICCCA)*, 2020.
- [18] M. D. MacKinley, K. A. Remley, M. Myslinski, J. S. Kenney, D. Schreurs, and B. Nauwelaers, "EVM calculation for broadband modulated signals," *ARFTG Microwave Measurement Conference*, 2004.
- [19] R. A. Shafik, M. S. Rahman, and A. R. Islam, "On the Extended Relationships Among EVM, BER and SNR as Performance Metrics," in *International Conference on Electrical and Computer Engineering (ICECE)*, 2006.
- [20] G. Ungerboeck, "Channel coding with multi-level/phase signals," *IEEE Transactions on Information Theory*, vol. 28, no. 7, pp. 55–67, 1982.
- [21] R. J. Essiambre and R. W. Tkach, "Capacity Trends and Limits of Optical Communication Networks," *Proceedings of the IEEE*, vol. 100, no. 5, pp. 1035–1055, 2012.
- [22] D. A. A. Mello, A. L. N. Souza, J. D. Reis, J. C. M. Diniz, L. H. H. Carvalho, N. G. Gonzalez, J. R. F. Oliveira, D. S. Arantes, and M. H. M. Costa, "Parameter selection in optical networks with variable-code-rate transceivers," in *International Conference on Optical Network Design and Modeling (ONDM)*, 2015.
- [23] M. Ziari, V. Lal, P. Studenkov, H. Hodaie, T. Frost, C. Tsai, K. Hoshino, B. Behnia, R. Going, S. Wolf, S. Porto, M. Kuntz, T. Vallaitis, E. Souidi, J. Lavrencik, R. Salvatore, N. Modi, P. Abolghasem, M. Fisher, S. Murthy, S. Buggaveeti, R. Brigham, D. Pavinski, J. Zhang, J. Zhang, S. Corzine, P. Evans, V. Dominic, R. Maher, P. Mertz, S. Sanders, H. Sun, J. Osenbach, and P. Kandappan, "High-performance 100 Gbaud Coherent Photonic Modules," in *Optical Fiber Communications Conference (OFC)*, 2021.
- [24] A. L. Souza, D. A. A. Mello, and J. D. Reis, "Experimental Evaluation of Data-Aided and Non-Data-Aided Dynamic Equalization Algorithms for Low OSNR Regimes," in *International Microwave and Optoelectronics Conference (IMOC)*, 2015.